Interaction of Axin and Dvl-2 proteins regulates Dvl-2-stimulated TCF-dependent transcription

Matthew J.Smalley, Elizabeth Sara, Hugh Paterson[1], Stuart Naylor[2], David Cook, Hiran Jayatilake, Lee G.Fryer, Lisa Hutchinson[3], Michael J.Fry[3] and Trevor C.Dale[4]

Developmental Biology and [3]Signal Transduction Teams, Section of Cell Biology and Experimental Pathology, Toby Robins Breakthrough Breast Cancer Research Centre, [1]Section of Cell and Molecular Biology, Chester Beatty Laboratories, Institute of Cancer Research, 237 Fulham Road, London SW3 6JB and [2]Oxford Biomedica, Oxford Science Park, Oxford OX4 4GA, UK

[3]Corresponding author
e-mail: trevor@icr.ac.uk

M.J.Smalley, E.Sara and H.Paterson contributed equally to this work

Axin promotes the phosphorylation of β-catenin by GSK-3β, leading to β-catenin degradation. Wnt signals interfere with β-catenin turnover, resulting in enhanced transcription of target genes through the increased formation of β-catenin complexes containing TCF transcription factors. Little is known about how GSK-3β-mediated β-catenin turnover is regulated in response to Wnt signals. We have explored the relationship between Axin and Dvl-2, a member of the Dishevelled family of proteins that function upstream of GSK-3β. Expression of Dvl-2 activated TCF-dependent transcription. This was blocked by co-expression of GSK-3β or Axin. Expression of a 59 amino acid GSK-3β-binding region from Axin strongly activated transcription in the absence of an upstream signal. Introduction of a point mutation into full-length Axin that prevented GSK-3β binding also generated a transcriptional activator. When co-expressed, Axin and Dvl-2 co-localized within expressing cells. When Dvl-2 localization was altered using a C-terminal CAAX motif, Axin was also redistributed, suggesting a close association between the two proteins, a conclusion supported by co-immunoprecipitation data. Deletion analysis suggested that Dvl-association determinants within Axin were contained between residues 603 and 810. The association of Axin with Dvl-2 may be important in the transmission of Wnt signals from Dvl-2 to GSK-3β.
Keywords: β-catenin/GSK-3β/localization/luciferase assay

Introduction

The current model of the Wnt-signalling pathway suggests that in the absence of a Wnt signal, the serine/threonine kinase glycogen synthase kinase-3β (GSK-3β) phosphorylates β-catenin as part of a multiprotein complex which contains the GSK-3β, adenomatous polyposis coli (APC), Axin and β-catenin proteins. Phosphorylation targets β-catenin for ubiquitin-mediated degradation (Aberle *et al*., 1997; Orford *et al*., 1997). When the Wnt-signalling pathway is activated via ligand binding to Frizzled receptors, GSK-3β function is inhibited, and β-catenin accumulates and interacts with TCF/LEF-1 transcription factors to activate transcription from promoters containing TCF-binding sites (reviewed in Gumbiner, 1995; Peifer, 1995; Bienz, 1998; Dale, 1998). Although several lines of evidence support the role of Axin–APC–GSK-3β as a β-catenin turnover complex, little is known about the mechanisms by which upstream signals inhibit GSK-3β and/or Axin–GSK-3β function in β-catenin turnover. Genetic epistasis experiments (Hooper, 1994; Siegfried *et al*., 1994) suggest that GSK-3β down-regulation may be mediated by Dishevelled proteins (Dsh in *Drosophila*; XDsh in *Xenopus*; Dvl-1, -2 and -3 in mammalian systems).

The Dvl family of proteins have no known enzymatic functions but do have several potential interaction motifs, namely an N-terminal DIX domain, a central PDZ domain and a C-terminal DEP domain (Klingensmith *et al*., 1994; Sussman *et al*., 1994; Theisen *et al*., 1994; Axelrod *et al*., 1998). Ectopic expression of Dsh activated Wnt-dependent processes in *Xenopus* and *Drosophila* systems (Sokol *et al*., 1995; Yanagawa *et al*., 1995). In *Drosophila* cells lines, the DIX and PDZ domains were shown to be required for Armadillo (β-catenin) stabilization, whereas deletion of the XDsh PDZ domain prevented XDsh-dependent axis duplication and generated a dominant negative protein that was able to interfere with endogenous pathways (Yanagawa *et al*., 1995; Sokol, 1996). The DEP domain was not required for β-catenin stabilization in *Drosophila* cl-8 cells (Yanagawa *et al*., 1995), but was required for the establishment of ommatidial polarity during *Drosophila* eye development (Boutros *et al*., 1998; Cooper and Bray, 1999). A role for the DEP domain in this process probably reflects its involvement in an alternative Wnt-dependent 'tissue-polarity' pathway that branches downstream of Dsh and involves Rho and Jnk (Strutt *et al*., 1997; Boutros *et al*., 1998). Interestingly, Dsh, but not DshΔDEP, was recruited to the cell membrane in a Frizzled-dependent manner when co-injected in *Xenopus* blastocoelar cells (Axelrod *et al*., 1998).

Addition of soluble Wingless ligand to *Drosophila* cl-8 cells resulted in Dsh hyperphosphorylation and Armadillo stabilization. Overexpression of Dsh in the *Drosophila* S2 cell line also led to hyperphosphorylation and Armadillo stabilization. However, the role of Dsh phosphorylation in signalling is not yet clear, since Dfrz2 overexpression in S2 cells induced phosphorylation of endogenous Dsh without Armadillo stabilization (Yanagawa *et al*., 1995; Willert *et al*., 1997). At least one kinase which phosphorylates Dsh has been identified as casein kinase-2 (Willert *et al*., 1997).

Axin was first identified as the product of the murine

fused locus (Zeng *et al.*, 1997) and is closely related to the Axil/Conductin protein described recently (Behrens *et al.*, 1998; Yamamoto *et al.*, 1998). Axin contains binding regions for several proteins (Figure 2), namely APC (RGS homology domain), GSK-3β, β-catenin, PP2A$_c$ and Axin itself (DIX domain) (Ikeda *et al.*, 1998; Kishida *et al.*, 1998; Hsu *et al.*, 1999). Three endpoint assays have been used to study Axin function: β-catenin stabilization; TCF-dependent transcription; and axis duplication in *Xenopus*.

Overexpression of wild-type Axin or Conductin suppressed an existing Wnt signal. In transcriptional assays, both wild-type Axin and Axin lacking the first 299 residues (including most of the RGS domain) inhibited Wnt-1-stimulated TCF-dependent transcription in 293 cells (Sakanaka *et al.*, 1998). Overexpression of Axin or Conductin alone in APC-mutant SW480 cells reduced the constitutively high levels of β-catenin (Behrens *et al.*, 1998; Nakamura *et al.*, 1998) and resulted in the suppression of TCF-dependent transcription (Sakanaka *et al.*, 1998). Expression of Axin or Conductin in *Xenopus* dorsal blastomeres prevented formation of the endogenous axis (Zeng *et al.*, 1997; Behrens *et al.*, 1998) in a process that could be relieved by co-expression of β-catenin, but not XWnt-8. This suggested that Axin functioned downstream of Wnt, but upstream of β-catenin (Zeng *et al.*, 1997). Dorsal microinjection of murine *Axin* mRNA with a C-terminal truncation at residue 724 (lacking the DIX domain and part of the PP2A$_c$-binding domain) also blocked *Xenopus* endogenous axis formation (Itoh *et al.*, 1998).

Mutants of Axin were also shown to activate downstream Wnt-dependent processes in the absence of a Wnt signal. In contrast to mammalian studies, deletion of the Axin RGS or DIX domains in *Xenopus* resulted in active proteins able to induce an ectopic ventral axis (Zeng *et al.*, 1997; Itoh *et al.*, 1998). In Neuro 2A cells, deletion of the APC, GSK-3β and β-catenin binding regions from Conductin stabilized β-catenin (Behrens *et al.*, 1998).

In this paper we describe the use of a domain-deletion and domain-expression approach to study the relationship between Axin, Dvl-2 and GSK-3β. The results support a function for GSK-3β downstream of Dvl-2 in a mammalian system. Our data more precisely delineate the GSK-3β-binding domain of Axin and suggest a role for the N-terminal region, including the RGS motif, which is independent of APC. We show that the introduction of a mutation into the GSK-3β-binding domain of Axin prevents GSK-3β–Axin interaction and turns Axin into a transcriptional activator. Finally, we demonstrate that Axin and Dvl-2 can direct each other's cellular localization and co-immunoprecipitation data suggest a physical association between the two proteins.

Results

GSK-3β and Axin interfere with Dvl-2-dependent TCF transcription

Expression of Wnt-1 in 293 cells (Sakanaka *et al.*, 1998) and Rat-1 fibroblasts (Young *et al.*, 1998) activated TCF-dependent transcription. To address whether Dvl-2 (the closest of the three mammalian homologues to *Drosophila* Dishevelled) activated the Wnt signal transduction pathway in mammalian cells, we used a transient-transfection reporter assay to measure TCF-dependent transcription. Fetal human kidney 293 epithelial cells were transfected with plasmids containing multimeric TCF- or mutant TCF-binding sites upstream of a basal c-*fos*-luciferase reporter gene (TOPFLASH and FOPFLASH; Korinek *et al.*, 1997). As described previously, co-transfection of a dominantly active β-catenin mutant (ΔN-β-catenin) strongly increased transcription from TOPFLASH compared with FOP-FLASH (data not shown). Ectopic expression of murine Dvl-2 stimulated TCF-dependent transcription in a concentration-dependent manner up to 50-fold within the range of protein expression levels tested (Figure 1A). Results were similar for hemagglutinin (HA)-tagged Dvl-2 (data not shown).

Genetic epistasis in *Drosophila* predicted that zw-3/sgg (GSK-3β) functions downstream of Dsh (Hooper, 1994; Siegfried *et al.*, 1994). However, this has not been demonstrated directly in a mammalian system. We therefore tested whether overexpression of GSK-3β could block Dvl-2-activated, TCF-dependent transcription (Figure 1B). When Dvl-2 and wild-type GSK-3β (GSK-3β wt) were co-expressed, Dvl-2-activated TCF-dependent transcription was suppressed by up to 50%, supporting a role for GSK-3β function downstream from, or parallel and dominant to, that of Dvl-2. Co-expression of Dvl-2 with the kinase-dead GSK-3β K85M mutant had no effect on Dvl-2-activated TCF-dependent transcription, supporting the current model of Wingless signalling that the kinase activity of GSK-3β may be required to inhibit TCF-dependent transcription. When Dvl-2 was co-expressed with a constitutively active mutant variant of GSK-3β, which had the regulatory serine at position 9 mutated to an alanine (GSK-3β S9A), transcription was suppressed by >80%. Phosphorylation of Ser9 by factors such as PKB and p90rsk-1 has been shown to inhibit GSK-3β activity in other systems (Stambolic and Woodgett, 1994; Cross *et al.*, 1995). None of these GSK-3β constructs had any effect on TCF-dependent transcription when expressed alone (Figure 1B). Interestingly, although the wild-type GSK-3β and GSK-3β S9A proteins appeared to be distributed equally between the pellet and supernatant fractions, the GSK-3β K85M was found principally in the supernatant (Figure 1B).

As Axin has been shown to inhibit Wnt-1-induced TCF-dependent transcription (Sakanaka *et al.*, 1998), we investigated whether it could also block Dvl-2-activated TCF-dependent transcription. We used form 1 Axin, which lacks the residues 36 amino acids found in form 2 (Figure 2; Zeng *et al.*, 1997). As shown in Figure 1C, full length, Flag-tagged murine Axin [mFlagAx-(1–956)] inhibited Dvl-2-activated, TCF-dependent transcription in a dose-dependent manner, but did not alter basal levels of TCF-dependent transcription (Figure 3B, second bar). To localize the regions of Axin that interfered with TCF-dependent transcription, we expressed a series of Flag-epitope-tagged Axin deletion proteins (Figure 2; results summarized in Table I). With the exception of mFlagAx-(Δ662–723), the truncated Axin proteins had a reduced ability to interfere with Dvl-2-activated transcription when compared with the wild type. An N-terminal Axin deletion, lacking the APC-binding region [mFlagAx-(351–956)], was a weak inhibitor of Dvl-2-activated transcription. This
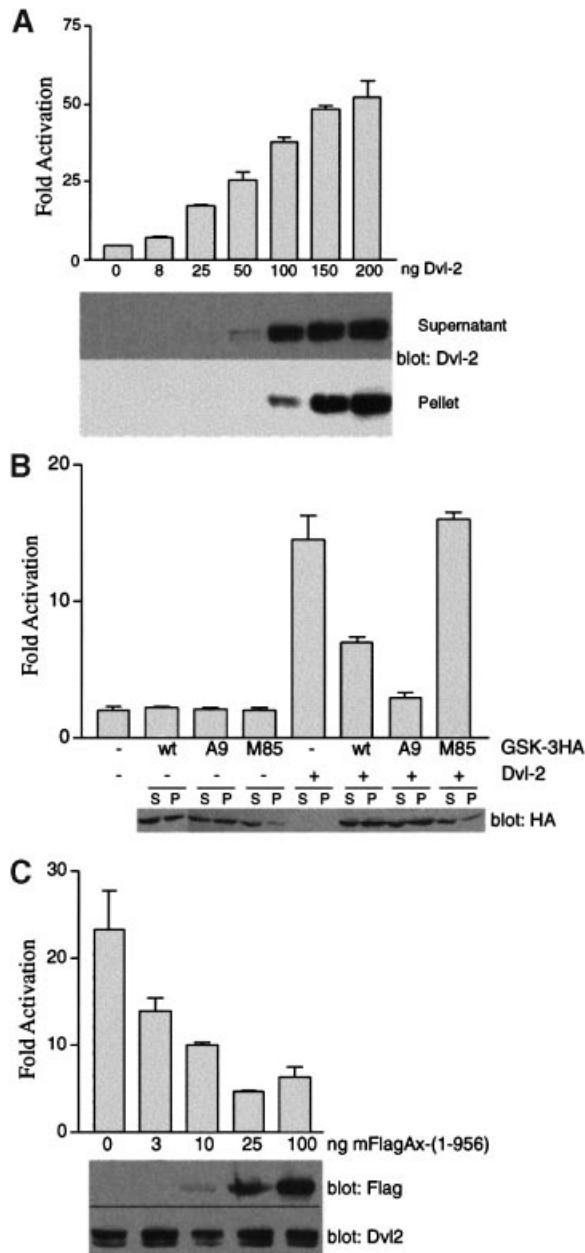
Fig. 1. GSK-3β and Axin inhibit Dvl-2 regulation of TCF-dependent transcription. (**A**) Concentration-dependent activation of transcription by Dvl-2 from a promoter containing multimerized TCF-binding sites. Fold activation is a ratio of expression from luciferase reporter constructs containing promoters with wild-type or mutant TCF-binding sites. Expression of Dvl-2 at each of the concentrations of transfected plasmid is illustrated by the accompanying immunoblot. (**B**) The effect of GSK-3βHA and mutants on Dvl-2 activated transcription. One hundred nanograms of each plasmid were transfected. The accompanying immunoblot shows the expression of the GSK-3β HA variants in the supernatant (S) or pellet (P) fractions. (**C**) Axin inhibition of Dvl-2-activated transcription. An immunoblot showing expression from the Flag-tagged Axin and Dvl-2 is shown.

Table I. Summary of activity of Axin proteins

Construct	Activity		
	Activation	Dvl-signal inhibition	Co-localization
FlagAx-(1–956)	–	strong	yes[b]
FlagAx-(1–956)–L521P	+++	nt	nt
FlagAx-(351–956)	–	weak	yes[b]
FlagAx-(351–956)–L521P	++++	nt	nt
FlagAx-(602–956)	–	–	yes[b]
FlagAx-(811–956)	–	–	no
FlagAx-(867–956)	–	–	nt
FlagAx-(1–810)	–	nt	yes
FlagAx-(1–810)–L521P	++	nt	yes
FlagAx-(1–477)	+	–	no
FlagAx-(368–701)	+	–	nt
FlagAx-(368–701)–L521P	–	nt	no
FlagAx-(501–560)	++++	–	nt
FlagAx-(501–560)–L521P	–	–	nt
FlagAx-(560–622)	–	–[a]	nt
FlagAx-(622–701)	–	–	nt
FlagAx-(196–354)	–	–[a]	nt
FlagAx-(Δ662–723)	–	strong	yes

Activation assays: –, no activation relative to TCF only control; +, 2- to 5-fold activation; ++, 5- to 10-fold activation; +++, 12- to 20-fold activation; ++++, 20- to 40-fold activation. Two methods were used to allow cross-comparison. First, activation was compared relative to Δ-Nβ-catenin, which was used as a positive control in most TCF-transcription assays. Secondly, protein expression from activating constructs was cross-compared within a single TCF-transcription assay (data not shown). [a]Co-operated with Dvl-2 to increase TCF-dependent activity. Co-localization: [b]Assayed with both HA-Dvl2 and HA-Dvl2-CAAX. nt, not tested.

generated a dominantly active protein in *Xenopus* studies. A C-terminally deleted Axin lacking the DIX domain [mFlagAx-(1–810)] had little or no effect on TCF-dependent transcription, neither interfering with HA-Dvl-2-activated transcription nor acting as a transcriptional activator (Figure 3B, bars three to five; Table I). In contrast, C-terminal deletions (of residues 725–992 and 812–992 of form 2 Axin, both including the DIX domain) did not interfere with the ability of Axin to prevent endogenous axis formation in *Xenopus* (Itoh *et al*., 1998).

Two regions of Axin behaved as activators of TCF-dependent transcription in our assays, mFlagAx-(1–477) and mFlagAx-(368–701) (Figure 4A; Table I). The N-terminal mFlagAx-(1–477) region lacked all recognized binding sites except for the RGS domain and might therefore function by titrating APC. The central mFlagAx-(368–701) region lacked both the APC-binding region and the DIX domain but contained the GSK-3β- and β-catenin-binding regions. The mFlagAx-(1–810) protein, which contained both the mFlagAx-(1–477) and mFlagAx-(368–701) regions, might have been expected to be a stronger activator than either alone. However, this was not the case (Table I), possibly because mFlagAx-(1–810) contained all the regions implicated in β-catenin turnover and may have retained residual ability to prevent β-catenin stabilization.

Expression of the conserved RGS [mFlagAx-(196–354)] or DIX domains [mFlagAx-(903–956)], or expression of the DIX plus PP2Ac-binding domains [mFlagAx-(602–956)] failed to activate or interfere with HA-Dvl-2-activated TCF-dependent transcription at a range of expression
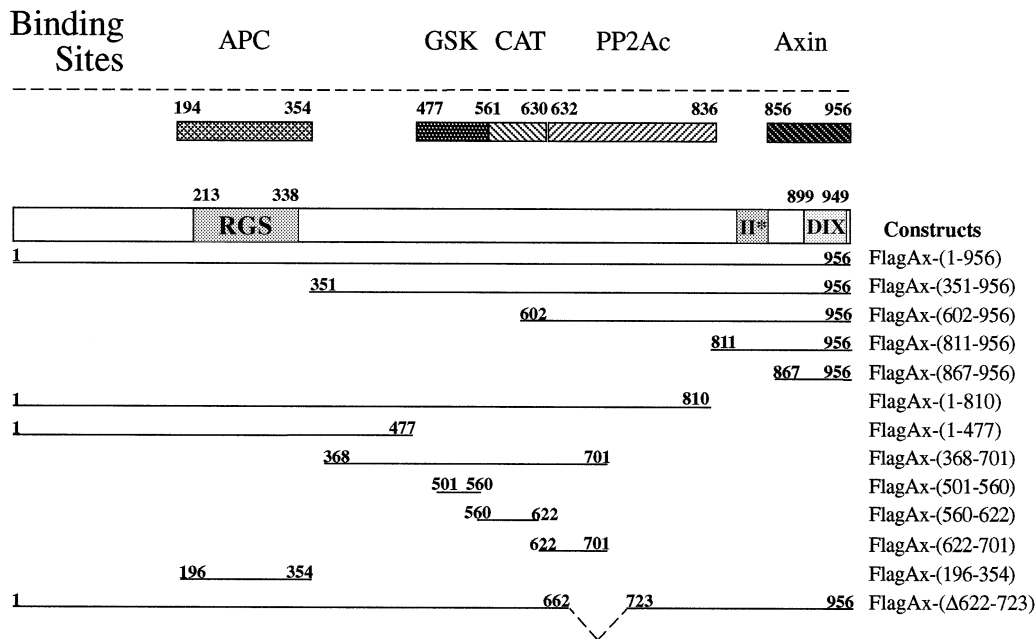
result contrasted with a similar N-terminal deletion of Axin (residues 1–288, including part of the RGS domain), which resulted in a protein with an increased ability to interfere with Wnt-1-dependent transcription in 293 cells (Sakanaka *et al*., 1998). mFlagAx-(351–956) showed no significant transcriptional activation when expressed alone (Figure 3A, second bar), in contrast to studies reported by Itoh *et al*. (1998) where a deletion of the RGS domain

Fig. 2. Diagrammatic representation of Axin fusion proteins and deletion constructs. Binding sites as defined by Hart *et al.* (1998), Ikeda *et al.* (1998) and Hsu *et al.* (1999) are illustrated as they correspond to the mouse Axin (Form 1 sequence co-ordinates). Form 2 contains a 36 amino acid insert shown by II*. Form 2 was not used in the studies presented here.

Fig. 3. TCF-dependent transcriptional regulation by truncated Axin proteins with and without the L521P mutation. (**A**) N-terminal truncation, mFlagAx-(351–956). (**B**) C-terminal truncation mFlagAx-(1–811). Fold activation as described in the legend to Figure 1. Expression of transfected constructs is shown by immunoblot against Flag epitope.

levels (Table I). No single recognizable domain of Axin was found to be sufficient to interfere with Dvl-2-activated transcription. However, two proteins were found to activate transcription when expressed alone, the central region of Axin, containing the GSK-3β- and β-catenin-binding domains, being the most active.

A 59 amino acid region from Axin activates TCF-dependent transcription

To localize the central region of Axin that activated TCF-dependent transcription, we made three epitope-tagged deletion proteins based on secondary structure predictions. Expression of a 59 amino acid region [mFlagAx-(501–560)] containing a putative coiled-coil motif (SMART program; Schultz *et al.*, 1998), strongly activated TCF-dependent transcription (Figure 4B). Expression of the β-catenin-binding region mFlagAx-(560–622) and mFlagAx-(622–701) failed to activate TCF-dependent transcription and did not interfere with Dvl-2-induced transcription (Table I).

As an independent confirmation that mFlagAx-(501–560) was acting to stimulate TCF-dependent transcription through endogenous components of the Wnt-signalling pathway, we expressed the protein in Neuro 2A cells and demonstrated that cells expressing mFlagAx-(501–560) accumulated high levels of nuclear β-catenin (Figure 4C; Behrens *et al.*, 1998).

The mFlagAx-(501–560) sequence is contained within a conserved GSK-3β-binding region in rat Axin, as defined by Ikeda *et al.* (1998), corresponding to the murine Axin residues 478–562. This contains no consensus GSK-3β phosphorylation sites, yet GSK-3β kinase activity has been shown to be required for binding to Axin (Ikeda *et al.*, 1998). When lysates of cells expressing mFlagAx-(501–560) were immunoprecipitated with anti-Flag antibodies, endogenous GSK-3β was co-precipitated with mFlagAx-(501–560), showing that the 59 residues of Axin were suffi-
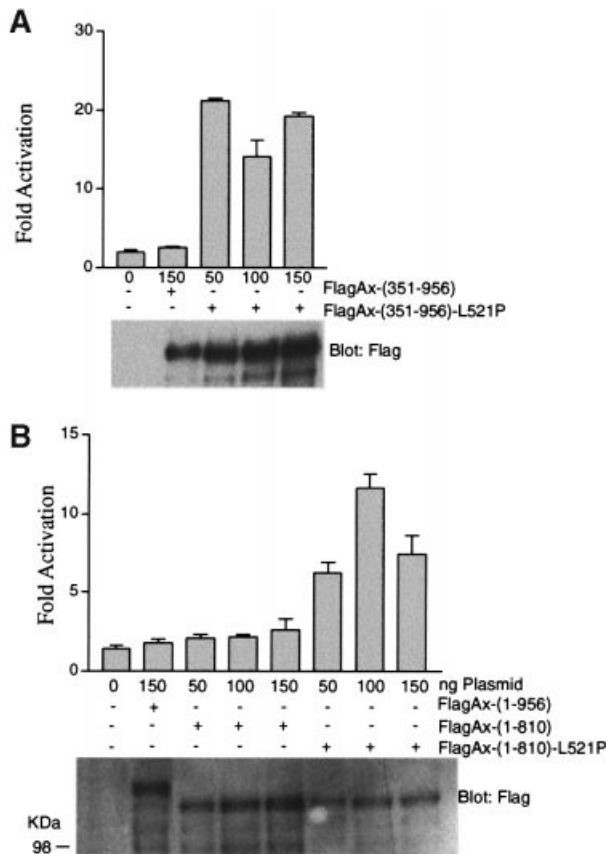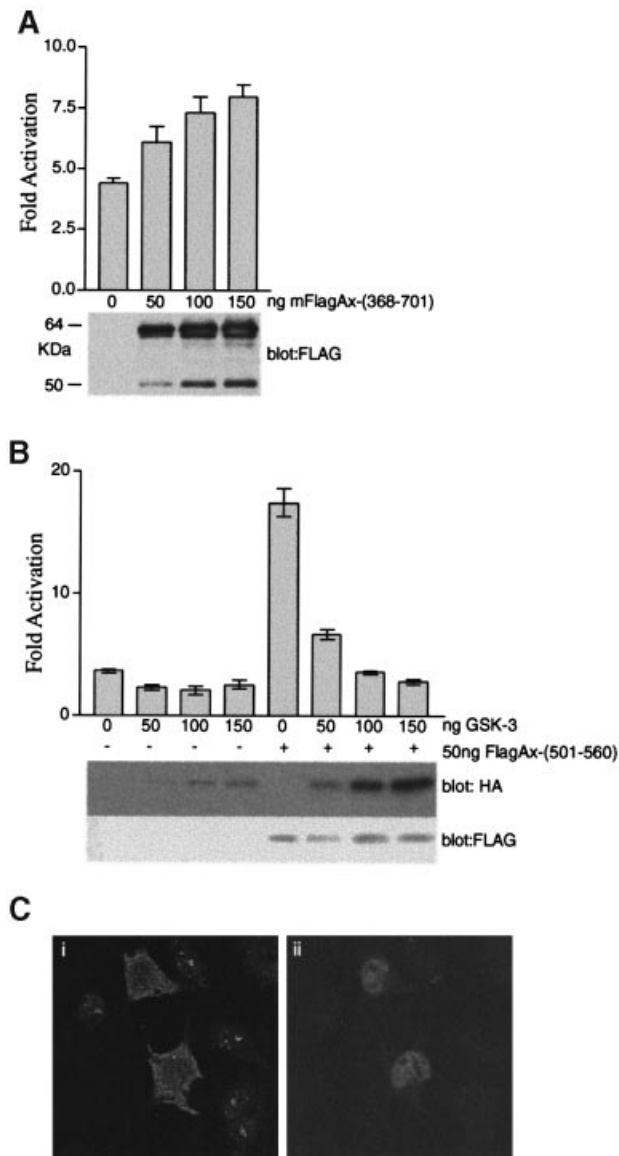
Fig. 4. Activation of TCF-dependent transcription by regions of Axin. (**A**) FlagAx-(368–701)-dependent activation of TCF-dependent transcription. Immunoblot analysis revealed a band of the expected size at 64 kDa, together with a smaller band at 50 kDa. (**B**) FlagAx-(501–560) strongly activated TCF-dependent transcription, whereas co-expression of GSK-3β reversed the induction. Immunoblots show GSK-3HA and FlagAx-(501–560) expression. Fold activation is as described in the legend to Figure 1. (**C**) Stabilization of endogenous β-catenin following transfection of FlagAx-(501–560) into Neuro 2A cells. (i) Flag detection; (ii) β-catenin detection.

cient for GSK-3β interaction (Figure 5A). One mechanism by which mFlagAx-(501–560) could function as an activator of TCF-dependent transcription could be the titration of GSK-3β from endogenous Axin complexes, thus preventing β-catenin turnover. A prediction from this model would be that mFlagAx-(501–560) activation of TCF-dependent transcription should be titrated by GSK-3β. Indeed, increasing HA-GSK-3β levels inhibited mFlagAx-(501–560)-induced TCF-dependent transcription in co-transfection experiments, suggesting that mFlagAx-(501–560) activation of TCF-dependent transcription was dependent on its interaction with GSK-3 (Figure 4B).

To confirm that the ability of mFlagAx-(501–560) to activate TCF-dependent transcription was dependent on its ability to bind GSK-3β, a leucine→proline mutation was introduced into the putative hydrophobic interface of the coiled-coil domain at position 521. An analogous mutation was previously shown to interfere with coiled-coil interactions between yeast MATa*1 and MATα2* *proteins (Johnson et al.,* 1998). In mFlagAx-(501–560), this substitution prevented GSK-3β binding (Figure 5A) and also changed the mobility and stability of the protein (Figure 5A and C). The P521 variant of mFlagAx-(501–560) migrated at a size consistent with its theoretical molecular weight both in transfected cells and in *in vitro* translations (data not shown). The L521P mutation did not affect the stability of the other Flag-Axin proteins into which it was introduced (Figure 5B; also Figure 3A and B). mFlagAx-(501–560)–L521P was unable to activate TCF-dependent transcription (Figure 5C), possibly because of its lower levels of expression than the wild-type equivalent or due to its inability to bind GSK-3β. We favour the latter model principally for two reasons. First, mFlagAx-(501–560) could activate transcription by up to 20-fold when cells were transfected with as little as 5 μg DNA per well (one-tenth of the smallest amount shown in Figure 5C). Secondly, when the L521P mutation was introduced into the construct covering the central region of Axin, which contained the GSK-3β- and β-catenin-binding regions [mFlagAx-(368–701)], the protein failed to activate TCF-dependent transcription and lost the activating potential of its parent (Table I). However, unlike mFlagAx-(501–560)–L521P, there was no gross difference in the levels of expression of mFlagAx-(368–701)–L521P and its parent protein (data not shown).

The L521P mutation transforms full-length Axin into a transcriptional activator

Next we investigated the effect of the L521P mutation in other Axin constructs. Full-length Axin did not activate TCF-dependent transcription, but unexpectedly, the introduction of L521P into full-length Myc- or Flag-tagged murine Axin [mFlagAx-(1–956)] transformed it into a transcriptional activator (Figure 5D). An N-terminal deletion lacking the RGS domain but containing the L521P mutation [mFlagAx-(351–956)–L521P] and a C-terminal deletion construct, which removed the DIX domain and contained the L521P mutation [mFlagAx-(1–810)–L521P], were also activators of TCF-dependent transcription, whereas the parent proteins were inactive (Figure 3A and B).

Immunoprecipitation experiments on lysates from cells transiently transfected with mFlagAx-(351–956), mFlagAx-(351–956)-L521P, mFlagAx-(1–810) or mFlagAx-(1–810)–L521P demonstrated that, as with mFlagAx-(501–560)–L521P, the mutation prevented mFlagAx-(351–956)–L521P and mFlagAx-(1–810)–L521P from interacting with endogenous GSK-3β (Figure 5B). Proteins with wild-type and mutant GSK-3β-binding sites were equally stable.

In summary, we identified an activating function of Axin that does not require the RGS domain, GSK-3β binding or the DIX domain. We also demonstrated that the PP2A$_c$-binding region plus DIX domain [mFlagAx-(602–956)] were not sufficient to substitute for this activity (Table I). The data suggest that this activity is a function
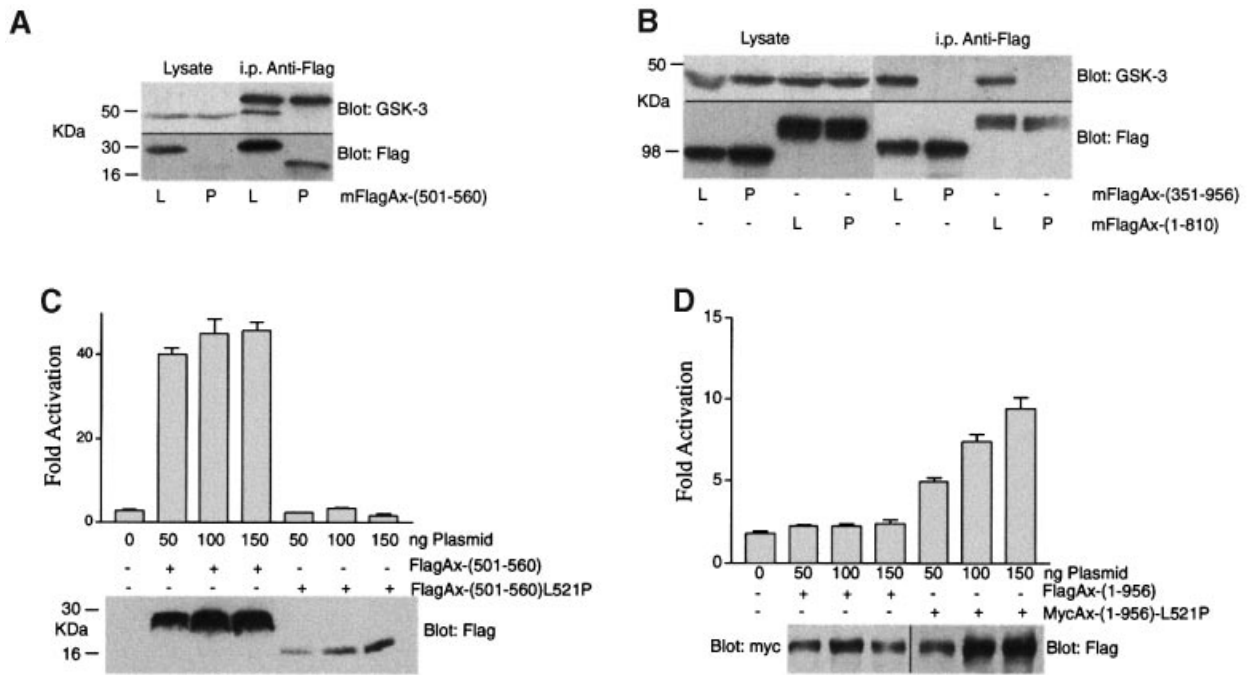
Fig. 5. The L521P mutation prevents GSK-3β association with Axin. (**A**) Immunoprecipitation of mFlagAx-(501–560) wild-type L521 or mutant P521 proteins; probed for endogenous GSK-3β. The top band in the third and fourth lanes (upper panel) is mouse immunoglobulin used in the immunoprecipitation. (**B**) Immunoprecipitation of wild-type L521 or mutant P521 variants of both mFlagAx-(1–956) and mFlagAx-(1–956) proteins; probed for endogenous GSK-3β. (**C**) Regulation of TCF-dependent transcription by mFlagAx-(501–560) and mFlagAx-(501–560)-L521P. (**D**) Activation of TCF-dependent transcription by mFlagAx-(1–956)-L521P. Fold activation is as described in the legend to Figure 1.

of the region lying between residues 351 and 810, and may require the interaction of multiple regions.

Subcellular localization of full-length Axin and Axin mutants

MDCK cells were microinjected with Flag-Axin constructs and the cells stained for expression after 2 h. At this time, full-length Flag-Axin [mFlagAx-(1–956)] was principally localized to a perinuclear region where it appeared to form irregular, non-vesicular masses (Figure 6A). To some extent this was dependent on the density of the cells and the time after microinjection, since Axin was also found localized adjacent to the plasma membrane in more densely packed cells and after longer periods of expression (data not shown). There was no cross-reactivity of the anti-Flag antibody or second antibody with endogenous or non-Flag-tagged exogenous proteins (Figure 7A).

When the Flag-Axin truncation proteins were microinjected, a range of localization patterns was observed. Note that in all cases, localization of the L521P variants was identical to that of the parent deletion protein. Microinjected mFlagAx-(351–956), which lacks the N-terminal RGS homology domain, localized to distinct, large cytoplasmic vesicles (Figure 6B). N-terminal deletion to amino acid 602 [mFlagAx-(602–956)] resulted in a protein localized with a punctate distribution that was not so clearly vesicular (Figure 6C). Further N-terminal deletions [mFlagAx-(811–956) and mFlagAx-(903–956)] gave diffuse cytosolic staining patterns (Figure 6D and E). A C-terminal Axin deletion that lacked the DIX domain [mFlagAx-(1–810)] had a diffuse cytosolic pattern of expression with some areas of particulate or vesicular staining (Figure 6F). mFlagAx-(1–477), which had a large

C-terminal deletion and retained only the RGS domain, showed a diffuse cytoplasmic pattern in some cells and nuclear staining in others (Figure 6G). The central region of Axin containing both GSK-3β- and β-catenin-binding regions [mFlagAx-(368–701)] showed diffuse cytoplasmic staining, but occasionally appeared to be present at or under the cell membrane in highly expressing cells (Figure 6H). mFlagAx-(Δ662–723) had a distribution identical to wild-type Flag-Axin (Figure 6I). The GSK-3β-binding domain from Axin [mFlagAx-(501–560)] was found to localize with a cytosolic pattern (Figure 6J). In summary, the data indicated that both N- and C-termini were required for wild-type Axin localization, but that the DIX and RGS homology motifs alone were incapable of specific localization.

The N-terminal, Axin RGS domain has been shown to be required for binding to APC (Hart *et al*., 1998; Kishida *et al*., 1998). To test whether APC was required for Axin localization, full-length mFlagAx-(1–956) and N-terminally deleted mFlagAx-(351–956) Axin expression constructs were microinjected into SW480 cells, which contain a truncated APC that was shown to be incapable of binding Axin (Kishida *et al*., 1998). The staining pattern of full-length Axin in SW480 cells was similar to that observed in MDCK cells (Figure 6A), showing that APC-independent localization determinants must be present within the N-terminal region of Axin (Figure 6K and L).

Axin and Dvl-2 co-localization

We examined the localization of HA-Dvl-2 and the various Flag-Axin deletion proteins in microinjected MDCK cells using multiple indirect immunofluorescence. All constructs were expressed for 2 h following microinjection. At this
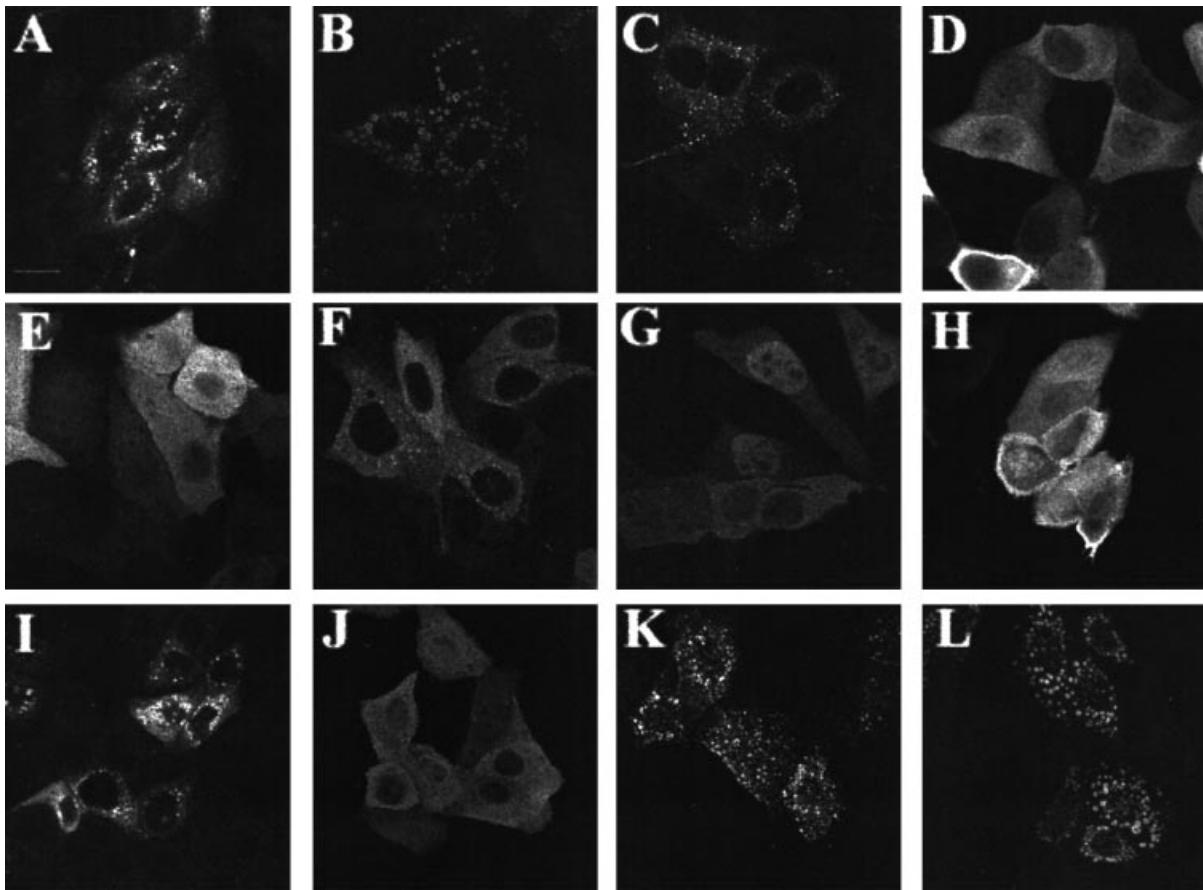
Fig. 6. Localization of Flag-Axin deletion proteins in MDCK (A–J) and SW480 cells (K, L). (**A**) mFlagAx-(1–956). (**B**) mFlagAx-(351–956). (**C**) mFlagAx-(602–956). (**D**) mFlagAx-(811–956). (**E**) mFlagAx-(903–956). (**F**) mFlagAx-(1–811). (**G**) mFlagAx-(1–477). (**H**) mFlagAx-(368–701). (**I**) mFlagAx-(Δ662–703). (**J**) mFlagAx-(501–560). (K, L) Localization of Flag-Axin deletion proteins in SW480 cells. (**K**) mFlagAx-(1–956). (**L**) mFlagAx-(351–956). Bar, 10 μm.

time, HA-Dvl-2 was localized to distinct cytoplasmic vesicles, which varied in size between cells (Figures 7B and 8A). The size of the vesicles appeared to correlate with the degree of expression of the protein, with the most strongly expressing cells having the largest vesicles. The staining pattern resembled that of the N-terminally deleted mFlagAx-(351–956).

To study the origin of the HA-Dvl-2 vesicles, an HA-Dvl-2–GFP fusion protein was generated to allow the visualization of vesicles in live cells. Time-lapse photomicroscopy showed that typically, HA-Dvl-2–GFP vesicles oscillated in real time over a distance of 1 or 2 μm but showed little sign of directed or consensus movement. When vesicles came into contact with each other, they frequently fused to form larger vesicles. There was no evidence for controlled 'streaming' of the vesicles (data not shown).

The similarities in the localization of HA-Dvl-2 and mFlagAx-(351–956) suggested that the two proteins might co-localize. We therefore examined cells co-injected with HA-Dvl-2 and Flag-Axin constructs. The results are summarized in Table I. Unexpectedly, wild-type Flag-Axin was found to exactly co-localize with HA-Dvl-2 (Figure 7E and F). The pattern of the co-localization generally resembled the perinuclear irregular masses seen previously with wild-type Flag-Axin alone, although some cells did have a co-localization pattern

which could be said to have been intermediate between the 'Axin' and 'Dvl-2' patterns. Controls demonstrated no cross-reactivity of either primary or secondary antibodies (Figure 7A and D). As expected, HA-Dvl-2 and N-terminal-deleted Flag-Axin [mFlagAx-(351–956)] also co-localized (Figure 7G and H).

To identify the region or regions of Axin mediating Dvl-2 co-localization, HA-Dvl-2 was co-expressed with the Flag-Axin deletion proteins. The mFlagAx-(603–956) (Figure 7I and J), mFlagAx-(1–811) (Figure 7K and L) and mFlagAx-(Δ662–723) (Figure 7M and N) proteins co-localized, whereas mFlagAx-(811–956) (Figure 7O and P), mFlagAx-(1–477) (Figure 7Q and R) and mFlagAx-(368–701)–L521P proteins failed to co-localize (Figure 7S and T). The overlap between regions of Axin that associated with HA-Dvl-2 suggest that sequences between residues 602 and 662 and/or between 723 and 810 were essential for co-localization. Interestingly, these regions overlap a region that was shown to bind PP2A$_c$, although the minimal PP2A$_c$-binding site was defined as being from residues 632–832, which extend C-terminally to the region shown to be sufficient for Dvl association in this study. Expression of the smallest construct that showed co-localization [mFlagAx-(602–956)] did not activate TCF-dependent transcription or inhibit Dvl-2-activated transcription (Table I).
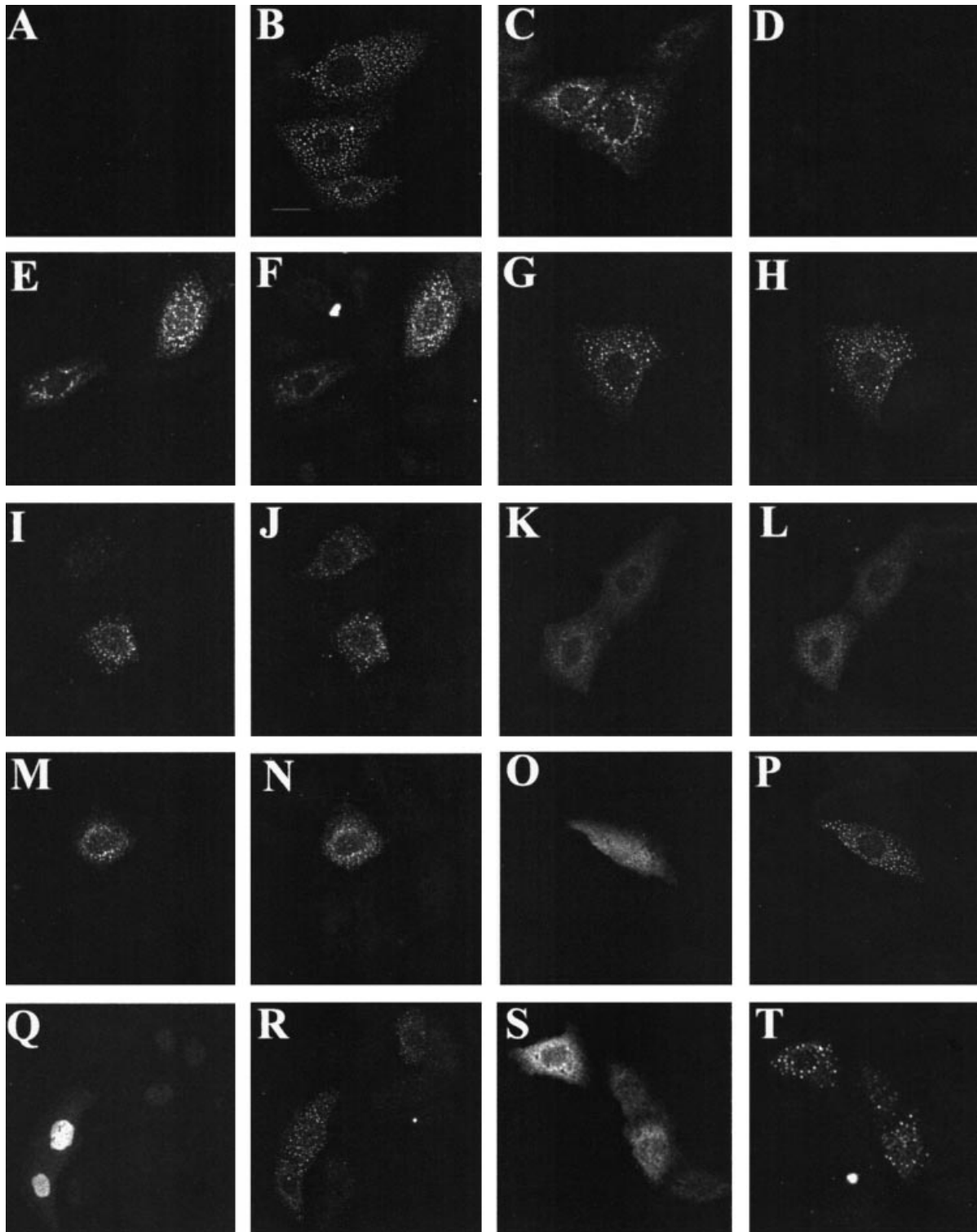
Fig. 7. Co-localization of HA-Dvl-2 and Flag-Axin deletion proteins in MDCK cells by double immunofluorescence. Flag epitope (mFlagAx constructs) is visualized in the first and third columns. HA epitope (HA-Dvl-2) is visualized in the second and fourth columns. (**A–D**) Cells microinjected with HA-Dvl-2 only (A, B) or mFlagAx-(1–956) only (C, D). Double staining demonstrates the lack of cross-reactivity by anti-HA and anti-Flag primary antibodies and their respective double antibodies. (E–T) Cells microinjected with both mFlagAx expression constructs and HA-Dvl-2. (**E**, **F**) mFlagAx-(1–956). (**G**, **H**) mFlagAx-(351–956). (**I**, **J**) mFlagAx-(602–956). (**K**, **L**) mFlagAx-(811–956). (**M**, **N**) mFlagAx-(1–811). (**O**, **P**) mFlagAx-(1–477). (**Q**, **R**) mFlagAx-(368–701). (**S**, **T**) mFlagAx-(Δ662–703). Bar, 10 μm.

HA-Dvl-2 and Flag-Axin association

Co-localization of Dvl-2 with Axin does not necessarily imply a direct interaction between the proteins, it could be a fortuitous event due to shared domains of common function. To address this problem, three of the Flag-Axin constructs were co-injected with an HA-Dvl-2 construct which contained the farnesylation signal from Ras at its C-terminus (HA-Dvl-2–CAAX; Aronheim *et al.*, 1994).

This resulted in the protein being redistributed within the cell, including being targeted to the plasma membrane (Figure 8A and B). If the co-localization of the Flag-Axin proteins and HA-Dvl-2 were the result of an association between the proteins, co-injection of the Flag-Axin and HA-Dvl-2–CAAX constructs should result in redistribution of both Axin and HA-Dvl-2–CAAX to new localization sites including the plasma membrane. As shown in Figure 8, this was indeed the case. Co-injection of HA-Dvl-2–CAAX with full-length Flag-Axin, mFlagAx-(351–956) or mFlagAx-(602–956) resulted in the redistribution and co-locaization of HA-Dvl-2–CAAX and the Flag-Axin. The co-localization at the plasma membrane was shown more clearly by false colour merging of highly co-expressing regions from Figure 8A and B (full-length Flag-Axin and HA-Dvl-2) Figure 8C and D (full-length Flag-Axin and HA-Dvl-2–CAAX). With this method, the distribution of the proteins was seen to be identical with both HA-Dvl-2 (Figure 9A) and HA-Dvl-2–CAAX (Figure 9B), and localized principally at the membrane with the latter.

Co-transfection of mFlagAx-(351–956) and HA-Dvl-2 followed by immunoprecipitation with an anti-HA antibody and subsequent Western blotting for Flag and HA epitopes, showed that mFlagAx-(351–956) was complexed with HA-Dvl-2 (Figure 9C), although the interaction was weak and with the reverse immunoprecipitation, using the anti-Flag antibody, we have so far been unable to detect mFlagAx-(351–956) complexed with HA-Dvl-2. mFlagAx-(351–956) was used in preference to full-length mFlagAx-(1–956) in immunoprecipitation experiments because we found that the wild-type protein was predominantly partitioned in the insoluble fraction following cell lysis (data not shown).

Discussion

The data presented here provide the first demonstration in mammalian cells of the regulation of TCF-dependent transcription (an endpoint of the Wnt-signalling pathway) by Dvl-2 expression. The data support existing models that place GSK-3β function downstream of, or in parallel and dominant to, Dvl, since expression of wild-type GSK-3β inhibited Dvl-2-activated transcription. A GSK-3β S9A mutant that prevents Ser9 phosphorylation was a more potent suppressor of the Dvl-2 signal than wild-type GSK-3β. As Ser9 is phosphorylated in response to ligands including insulin and EGF (Saito *et al.*, 1994; Cross *et al.*, 1995; Eldar-Finkelman *et al.*, 1995), the effects of GSK-3β S9A on Dvl-2-activated transcription suggest that Ser9 may also be of importance during Wnt inhibition of GSK-3β activity (Cook *et al.*, 1996), or for cross-talk between Wnt and other signalling pathways.

The K85M mutation in the ATP-binding site of GSK-3β renders it catalytically inactive. GSK-3β K85M was neutral in our assays, having no effect on TCF-dependent transcription or blocking Dvl-2-activated transcription. This was surprising, as the same mutation functioned as a dominant activator of Wnt signalling in *Xenopus*, as shown by the induction of an ectopic axis (He *et al.*, 1995). The reason for the difference between the *Xenopus* and mammalian systems is unclear. However, GSK-3β K85M has been reported to not bind Axin following
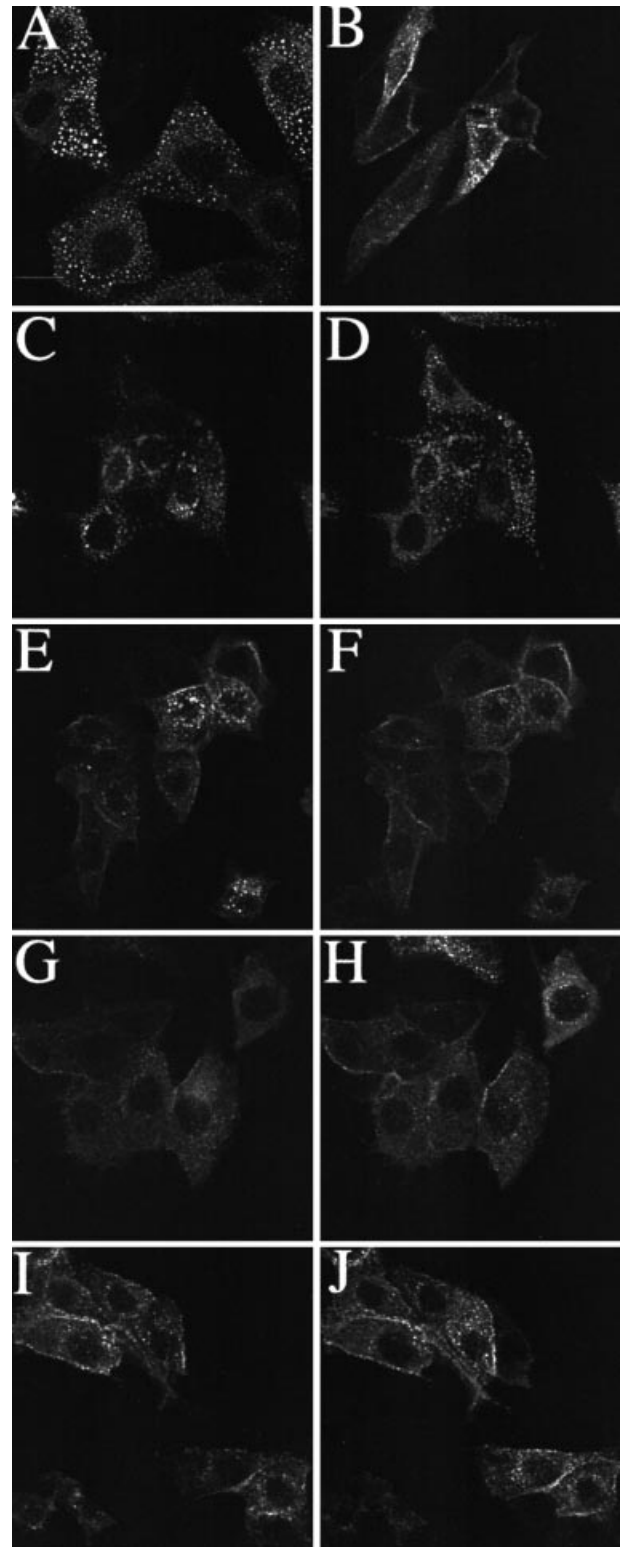

Fig. 8. Co-localization of HA-Dvl-2-CAAX and Flag-Axin deletion proteins in MDCK cells by double immunofluorescence. (A, B) Cells microinjected with (**A**) HA-Dvl-2 showing normal vesicular localization and (**B**) HA-Dvl-2–CAAX showing membrane as well as cytoplasmic localization. (C, D) Co-localization of (**C**) mFlagAx-(1–956) and (**D**) HA-Dvl-2 in previously observed 'Axin-like' staining pattern. (**E–J**) Cells microinjected with both mFlagAx expression constructs and HA-Dvl-2–CAAX showing co-localization at the membrane as well as in the cytoplasm. HA-Dvl-2 is shown in (F), (H) and (J). (**E**) mFlagAx-(1–956). (**G**) mFlagAx-(351–956). (**I**) mFlagAx-(602–956). Bar, 10 μm.
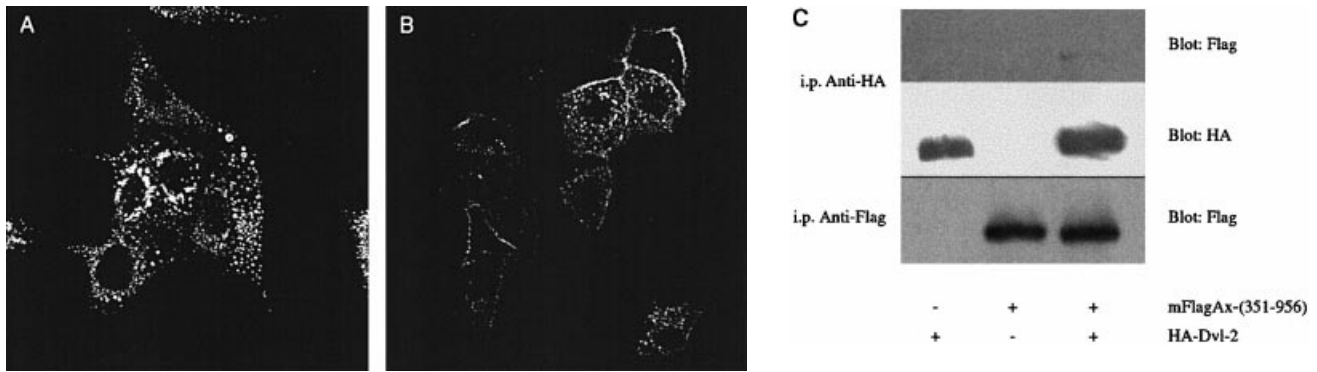
Fig. 9. Axin–Dvl association. (**A**) Co-localization of FlagAx-(1–956) and HA-Dvl-2. (**B**) Co-localization of FlagAx-(1–956) and HA-Dvl-2–CAAX. Data from Figure 8C and D and Figure 8E and F were processed by Bio-Rad Lasersharp software to illustrate areas of co-localization. The highest levels of expression were displayed as a colour image on a grey-scale background. (**C**) Immunoprecipitation of HA-Dvl-2 by association with FlagAx-(351–956).

transient transfection in COS cells (Ikeda *et al.*, 1998) suggesting that the function of GSK-3β K85M in *Xenopus* was not directly mediated by binding to Axin.

We have been able to localize more exactly the GSK-3β-binding region of Axin to residues 501–560. When mFlagAx-(501–560) was expressed alone, it strongly activated TCF-dependent transcription. This may be through the binding and titration of GSK-3β from an endogenous Axin–β-catenin turnover complex, since activation could be reversed by increasing GSK-3β levels. When a leucine→proline mutation was introduced at position 521, GSK-3β binding and TCF-dependent transcription were blocked, supporting a critical role for GSK-3β binding in the activation of transcription by mFlagAx-(501–560).

Unexpectedly, when the L521P mutation was introduced into full-length Flag-Axin, it generated an activator of TCF-dependent transcription. By introducing the L521P mutation into truncated Axin proteins, we demonstrated that the N-terminal, APC-binding RGS and C-terminal Axin-dimerization DIX domains were not required for the dominant-activating effect of the L521P mutation. Recent studies have also shown an activating function in mutants of Conductin/Axil which lack the APC, GSK-β- and β-catenin-binding regions (Behrens *et al.*, 1998). If this study depends on a similar mechanism of action, our data would also suggest that the DIX domain is not required for the activation of transcription. The inability of mFlagAx-(602–956) to activate TCF-dependent transcription also suggests that PP2A$_c$ titration could not account for transcriptional activation, although we have not proven that the mutant proteins retain the ability to bind PP2A$_c$ in our system. Detailed analysis of Axin deletion constructs will be required to define accurately the regions mediating activation by L521P mutant proteins. Our initial data suggest that residues 351–810 from the Axin L521P mutant proteins function to induce transcription and that none of the protein interaction regions identified previously are sufficient to induce this activity on their own.

Microinjection experiments localized Axin to perinuclear irregular masses. Deletion studies showed that both the N- and C-terminal domains were required for this distribution, as an N-terminal deletion including the RGS domain [mFlagAx-(351–956)] localized to large cytoplasmic vesicles, whereas a C-terminal deletion including

the DIX domain [mFlagAx-(1–810)] had a diffuse cytoplasmic localization with occasional vesicles.

As the RGS domain of Axin was shown to bind APC (Hart *et al.*, 1998; Kishida *et al.*, 1998), we considered the possibility that APC mediated the perinuclear localization of Axin. Full-length Axin retained a normal localization pattern in SW480 cells, which contain a deleted version of APC that is incapable of binding Axin (Hart *et al.*, 1998; Kishida *et al.*, 1998), suggesting that factors other than APC were important in Axin localization. Further studies should be able to delineate the regions mediating this localization and help determine whether Axin-localization and APC-binding determinants are discrete or overlap.

HA-Dvl-2 localized to cytoplasmic vesicles, the size of which depended on levels of protein expression. The vesicles appeared similar to RhoB vesicles observed previously (Adamson *et al.*, 1992), but did not co-stain with antibodies to RhoB (data not shown). The physiological relevance of the vesicles is unclear. Endogenous Dsh protein was detected in vesicles within late-stage imaginal discs; however, Dsh localization in the *Drosophila* ventral epidermis at times of active Wnt signalling had a diffuse cytoplasmic appearance (Yanagawa *et al.*, 1995). Previous overexpression studies in *Drosophila* S2 cells and *Xenopus* blastocoelar cells also showed Dsh localization in cytoplasmic vesicles (Axelrod *et al.*, 1996, 1998).

When Flag-Axin and HA-Dvl-2 proteins were co-expressed, they altered each other's localization, such that within each cell examined, their localization overlapped. In most cells the pattern of localization was reminiscent of that of Axin alone, although in some cases intermediate forms were seen, suggesting that Axin altered Dvl-2 localization and vice versa. It may be that the exact pattern was determined by the relative levels of expression of the two proteins. The specific nature of the Axin–Dvl-2 interaction was demonstrated by co-expression of Axin and Dvl-2 with the CAAX motif. Again, the localization of the two proteins overlapped exactly. Although our immunofluorescence data suggested that a large fraction of co-transfected Axin and Dvl-2 was complexed *in vivo*, we were only able to detect a small fraction of this complex by immunoprecipitation. The reason for the lability of Axin–Dvl-2 interactions in cell extracts is not clear at present.

The regions of Axin required for Dvl-2/Axin co-localization were defined by deletion analysis to lie C-terminal of amino acid 602 and N-terminal of amino acid 810. This region does not include the region binding GSK-3β, but does overlap with the recently identified PP2A$_c$-binding region of Axin (residues 632–836). There is therefore the possibility that Axin–Dvl-2 interactions are mediated via PP2A$_c$. However, mapping of the PP2A$_c$-binding region in a yeast two-hybrid assay suggested that loss of residues 811–836 significantly reduced the interaction of this region with PP2A$_c$, although it did not abolish it (Hsu et al., 1999). The relationship between Dvl-2 and PP2A$_c$ is therefore far from clear.

These data implicate Axin association in Wnt signal transmission from Dvl-2 to GSK-3β. It should be noted, however, that specific, Dvl/Dsh-mediated inhibition of Axin-associated GSK-3β function may not be a universal mechanism in Wnt signalling, as despite sequencing of the genome of Caenorhabditis elegans being effectively complete, no Axin homologues have been found, although it does contain Dsh, APC, GSK-3β and β-catenin homologues. It may be that the requirement for signalling specificity is reduced in C.elegans, or other proteins (perhaps APC) may fulfil the role of Axin.

There are broadly two classes of models into which the relationship between a Wnt signal and Dvl–Axin association may be grouped. First, Dvl–Axin association (or disassociation) may be inducible and Wnt (or other) signal dependent. If this is the case, the dynamic modulation of Dvl–Axin association may directly control the rate of β-catenin phosphorylation, either by altering the access of GSK-3β to β-catenin or by Dvl-recruiting activities which modulate GSK-3β activity. In this context, there is evidence for protein kinase C (PKC) function in Wingless signalling to GSK-3β (Cook et al., 1996), and certain PKC isoforms, such as PKCα, contain C-terminal S/T-X-V motifs that bind PDZ domains (Staudinger et al., 1997). Furthermore, GSK-3β (but not GSK-3α) is known to be an in vitro substrate for PKCα. Therefore, in this model, the role of Dvl-2 may be as an adapter protein that takes PKC to GSK-3β. As Dvl-2 and PP2A$_c$-binding regions of Axin (602–810 and 632–832 respectively) appear to overlap to some extent, there may be an additional role for Dvl-2 in the modulation of PP2A$_c$-binding function, or vice versa. We have also shown that the Axin DIX domain is not required for Dvl–Axin interaction. It remains possible that the interaction of Dvl-2 with Axin between residues 602 and 810 brings the DIX domain of Dvl-2 into close contact with that of Axin, promoting or disrupting their interaction. Alternatively, the DIX domain of Dvl-2 may simply serve to localize the protein to the same compartment as Axin, facilitating their interaction via other domains.

The second broad class of model would suggest that Dvl–Axin association is constitutive and signal independent. In this model, the question of how an Axin–β-catenin complex was regulated by Wnt signals would be changed to a question of how a constitutive Axin–Dvl–β-catenin complex was regulated. The data we have presented prove the association of Dvl–Axin but give no information on how the complexes receive a signal following ligand–receptor interaction, and thus cannot distinguish between the two models. Overexpression of proteins also makes it difficult to determine physiological mechanisms. Recent studies demonstrating Dsh recruitment to cell membranes following co-expression of Frizzled suggest that differential Dsh/Dvl association or localization with a range of signalling componants may be important for signal transmission (Axelrod et al., 1998). Studies examining the localization of endogenous Dsh/Dvl using biochemical methods have provided evidence for translocation of a small fraction of the endogenous Dsh/Dvl pool to membrane fractions (Yanagawa et al., 1995) or membrane and cytoskeletal fractions (Steitz et al., 1996) in response to Wingless/Wnt ligand. We have preliminary data confirming translocation of a minor fraction of endogenous Dvl-2 to P100 membrane fractions following treatment of murine fibroblasts with Wingless-conditioned medium (L.Hutchinson and M.Fry, unpublished results; data not shown). So far, we have not been able to visualize the relocalization of this signal-dependent subfraction by immunofluorescence.

We have shown that Axin has an activating function similar to that seen in Conductin/Axil protein deletions and have demonstrated that this function is unlikely to be mediated by any of the known interaction domains acting in isolation. We have also shown a direct interaction between Axin and Dvl-2, implicating a role for such an association in the transmission of the Wnt signal from Dvl-2 to GSK-3β. Further studies will shed more light on Axin function and on how Dsh/Dvl and Axin interact to control β-catenin turnover and provide specificity within the Wnt-signalling pathway.

Materials and methods

Preparation of Dvl-2, GSK-3 and Axin constructs
A murine Dvl-2 cDNA (obtained from D.Sussman) was tagged at the N-terminus with the HA epitope (YPYDVPDYA) using PCR methodology. The sequence (KLNPPDESGPGCMSCKCVLS) directing farnesylation and membrane localization was taken from Ha-ras (Aronheim et al., 1994) and added to the C-terminus of Dvl-2. Dvl-2-GFP was made by subcloning the HA-Dvl-2 sequence into pEGFP (Clontech). The HA-tagged GSK-3 mutants were made from pTM3β-tag (obtained from J.Woodgett). The insert was cloned into Bluescript, mutated using the QuikChange Site-directed Mutagenesis Kit (Stratagene) and the products cloned into the pcDNA3.1+ vector (Invitrogen). The full-length Axin constructs were subcloned from a Myc-tagged Axin Form 1 cDNA (obtained from F.Constantini) into the CMV expression vector pcDNA3.1+ which had been modified to include two FLAG epitope tags (DYKDDDDK; Stratagene). The N- and C-terminal deletion constructs were prepared using restriction endonucleases. The remaining constructs containing the putative binding domains were generated by PCR using the high-fidelity Pfu Turbo polymerase (Stratagene). The L521P mutants were made using the QuikChange mutagenesis kit.

Cell culture
Neuro 2A cells (obtained from EACC, Porton Down) were cultured in basal medium Eagle's (BME) supplemented with non-essential amino acids and 10% fetal calf serum at 37°C in 12% CO_2. SW480 and Madin–Darby Canine Kidney (MDCK) cells used for microinjection as well as 293 cells used for the luciferase assay were maintained in Dulbecco's modified Eagle's medium (DMEM) containing 10% FCS at 37°C in 12% CO_2.

Luciferase assay and Western analysis
293 cells were seeded at 7.5×10^4 cells/well in six-well dishes (NUNC), 48 h before an experiment. Each well was transfected with 0.5 µg of one of the luciferase reporters TOPFLASH or FOPFLASH (Korinek et al., 1997), 0.15 µg of CMV-hTCF4 (Korinek et al., 1997), 25 ng of CMV-lacZ as an internal control and the indicated amount of test construct(s). The CMV promoter-containing plasmid pcDNA3.1 (Invitrogen) was used to

equalize the total amount of CMV-driven plasmid per well. Carrier DNA (salmon sperm) was added to a total of 2 μg. Transfection was performed in triplicate using FuGENE 6 (Boehringer Mannheim) according to the manufacturer's instructions. Luciferase and β-galactosidase activity were measured 48 h later. For the luciferase assays, cells were harvested into phosphate-buffered saline (PBS) and pelleted with a low-speed spin. Cell pellets were then lysed with reporter lysis buffer and processed to generate cell supernatant and pellet fractions according to the manufacturer's recommendations (Promega Luciferase Assay system). Both fractions were kept for Western analysis. Luciferase activity in 20 μl of supernatant fraction was measured in an AutoLumat LB953 (Berthold). For the β-galactosidase activity measurements, 20 μl of the supernatant fractions were used in a spectrometric kinetic assay based on the substrate CPRG (Boehringer Mannheim). Fold-activation luciferase results were calculated after correcting for β-galactosidase by dividing the TOPFLASH values (TCF-binding motif) with those for FOPFLASH (mutant motif). For Western analysis, the triplicate samples containing TOPFLASH were combined and the supernatant and pellets run separately on SDS–PAGE gels after normalizing protein loading for β-galactosidase expression. Unless stated otherwise, only data from supernatant fractions are presented adjacent to the luciferase TCF-transcription assay data. Antibodies used were: mouse anti-HA monoclonal antibody (mAb) 12CA5, rat high-affinity anti-HA mAb (Boehringer Mannheim), anti-Dvl-2 (raised in rabbits against the C-terminus of GST-Dvl-2) and mouse anti-Flag M2 mAb (Sigma). Secondary antibodies used were against the appropriate species and horseradish peroxidase (HRP) conjugated for visualization with ECL Western Blotting detection reagents (Amersham Pharmacia Biotech). Immunoblots shown in the figures are of the supernatant fraction unless stated otherwise.

Stabilization of β-catenin in Neuro 2A cells

Neuro 2A cells were seeded on coverslips in 24-well plates at $1 \times 10^4 / cm^2$. After 48 h they were transfected using the FuGENE 6 method according to the manufacturer's protocol. After 24 h they were fixed in 2% (w/v) paraformaldehyde in PBS, permeabilized with 0.2% (v/v) Triton X-100 for 10 min and then stained by multiple indirect immunofluorescence (essentially according to Smalley *et al.*, 1998) for Flag-tagged proteins and endogenous β-catenin using polyclonal rabbit anti-Flag and mouse anti-β-catenin (Transduction Laboratories) mAb.

Immunoprecipitation

Cells were lysed with buffer containing 20 mM Triethanolamine (TEA) pH 9.2, 20 mM EDTA, Protease Inhibitor cocktail (Cat. no. P8340, Sigma), 20 μM chymostatin, 10 nm microcystin-LR, 10 mM dithiothreitol and 2% *n*-dodecyl-β-D-maltoside. (Previous assays with more physiological buffers had failed to extract full-length Axin protein into a soluble form.) The cell lysates were pre-cleared with 50 μl protein G–Sepharose beads (Amersham Pharmacia Biotech) for 30 min on a rotating wheel at 4°C. Aliquots containing 750 μg protein were made up to a volume of 500 μl and incubated, again on the rotating wheel at 4°C with 2 μg antibody for 2 h. Protein G–Sepharose beads (50 μl) were then added for a further incubation of 1 h. The beads were then pelleted and washed three times with lysis buffer and used for Western analysis. Antibodies used were anti-Flag M2 and anti-HA as used in immunoblotting.

Co-localization

Cells were grown to confluence on 60-mm dishes, microinjected with plasmids at a concentration of 50 μg/ml in PBS. After 4–6 h the cells were fixed in 4% (w/v) paraformaldehyde in PBS for 20 min. and permeabilized in 0.2% Triton X-100 for 15 min. Primary antibodies used were: rat anti-HA mAb (Boehringer Mannheim), mouse anti-Flag M2 and anti-myc 9E10 (Sigma). Where FITC or Texas Red-conjugated secondary antibodies (Jackson ImmunoResearch) were used, they were first pre-absorbed against the any other species of antibody (rat or mouse) to prevent cross-reaction. All antibodies were used at a working concentration of 10 μg/ml.

Acknowledgements

References

Aberle,H., Bauer,A., Stappert,J., Kispert,A. and Kemler,R. (1997) β-catenin is a target for the ubiquitin–proteasome pathway. *EMBO J.*, **16**, 3797–3804.

Adamson,P., Paterson,H.F. and Hall,A. (1992) Intracellular localization of the P21rho proteins. *J. Cell Biol.*, **119**, 617–627.

Aronheim,A., Engelberg,D., Li,N., al Alawi,N., Schlessinger,J. and Karin,M. (1994) Membrane targeting of the nucleotide exchange factor Sos is sufficient for activating the Ras signaling pathway. *Cell*, **78**, 949–961.

Axelrod,J.D., Matsuno,K., Artavanis-Tsakonas,S. and Perrimon,N. (1996) Interaction between Wingless and Notch signaling pathways mediated by Dishevelled. *Science*, **271**, 1826–1832.

Axelrod,J.D., Miller,J.R., Shulman,J.M., Moon,R.T. and Perrimon,N. (1998) Differential recruitment of Dishevelled provides signaling specificity in the planar cell polarity and Wingless signaling pathways. *Genes Dev.*, **12**, 2610–2622.

Behrens,J., Jerchow,B.A., Wurtele,M., Grimm,J., Asbrand,C., Wirtz,R., Kuhl,M., Wedlich,D. and Birchmeier,W. (1998) Functional interaction of an Axin homolog, Conductin, with β-catenin, APC and GSK-3β. *Science*, **280**, 596–599.

Bienz,M. (1998) TCF: transcriptional activator or repressor? *Curr. Opin. Cell Biol.*, **10**, 366–372.

Boutros,M., Paricio,N., Strutt,D.I. and Mlodzik,M. (1998) Dishevelled activates JNK and discriminates between JNK pathways in planar polarity and Wingless signalling. *Cell*, **94**, 109–118.

Cook,D., Fry,M.J., Sumatipala,R., Hughes,K., Woodgett,J.R. and Dale,T.C. (1996) Wingless inactivates glycogen synthase kinase-3 via an intracellular signalling pathway which involves a protein kinase C. *EMBO J.*, **15**, 4526–4536.

Cooper,M.T.D. and Bray,S. (1999) Frizzled regulation of Notch signalling polarises cell fate in the *Drosophila* eye. *Nature*, **397**, 526–530.

Cross,D.A.E., Alessi,D.R., Cohen,P., Andjelkovich,M. and Hemmings,B.A. (1995) Inhibition of glycogen synthase kinase-3 by insulin mediated by protein kinase B. *Nature*, **378**, 785–789.

Dale,T.C. (1998) Signal transduction by the Wnt family of ligands. *Biochem. J.*, **329**, 209–223.

Eldar-Finkelman,H., Seger,R., Vandenheede,J.R. and Krebs,E.G. (1995) Inactivation of glycogen synthase kinase-3 by epidermal growth factor is mediated by mitogen-activated protein kinase/p90 ribosomal protein S6 kinase signaling pathway in NIH/3T3 cells. *J. Biol. Chem.*, **270**, 987–990.

Gumbiner,B.M. (1995) Signal transduction by β-catenin. *Curr. Opin. Cell Biol.*, **7**, 634–640.

Hart,M.J., de los Santos,R., Albert,I.N., Rubinfeld,B. and Polakis,P. (1998) Downregulation of β-catenin by human Axin and its association with the APC tumour suppressor, β-catenin and GSK-3β. *Curr. Biol.*, **8**, 573–581.

He,X., Saint-Jeannet,J.-P., Woodgett,J.R., Varmus,H.E. and Dawid,I.B. (1995) Glycogen synthase kinase-3 and dorsoventral patterning in *Xenopus* embryos. *Nature*, **374**, 617–622.

Hooper,J.E. (1994) Distinct pathways for autocrine and paracrine Wingless signalling in *Drosophila* embryos. *Nature*, **372**, 461–464.

Hsu,W., Zeng,L. and Constantini,F. (1999) Identification of a domain of Axin that binds to the serine/threonine protein phosphatase 2A and a self-binding domain. *J. Biol. Chem.*, **274**, 3439–3445.

Ikeda,S., Kishida,S., Yamamoto,H., Murai,H., Koyama,S. and Kikuchi,A. (1998) Axin, a negative regulator of the Wnt signaling pathway, forms a complex with GSK-3β and β-catenin and promotes GSK-3β-dependent phosphorylation of β-catenin. *EMBO J.*, **17**, 1371–1384.

Itoh,K., Krupnik,V.E. and Sokol,S.Y. (1998) Axis determination in *Xenopus* involves biochemical interactions of Axin, glycogen synthase kinase-3 and β-catenin. *Curr. Biol.*, **8**, 591–594.

Johnson,P.R., Swanson,R., Rakhilina,L. and Hochstrasser,M. (1998) Degradation signal masking by heterodimerization of MATα2 and MAT**a**1 blocks their mutual destruction by the ubiquitin–proteasome pathway. *Cell*, **94**, 217–227.

Kishida,S., Yamamoto,H., Ikeda,S., Kishida,M., Sakamoto,I., Koyama,S. and Kikuchi,A. (1998) Axin, a negative regulator of the wnt signaling pathway, directly interacts with adenomatous polyposis coli and regulates the stabilization of β-catenin. *J. Biol. Chem.*, **273**, 10823–10826.

Klingensmith,J., Nusse,R. and Perrimon,N. (1994) The *Drosophila* segment polarity gene Dishevelled encodes a novel protein required for response to the Wingless signal. *Genes Dev.*, **8**, 118–130.

Korinek,V., Barker,N., Morin,P.J., van Wichen,D., de Weger,R., Kinzler,K.W., Vogelstein,B. and Clevers,H. (1997) Constitutive transcriptional activation by a β-catenin–TCF complex in APC⁻/⁻ colon carcinoma. *Science*, **275**, 1784–1787.

Nakamura,T., Hamada,F., Ishidate,T., Anai,K., Kawahara,K., Toyoshima,K. and Akiyama,T. (1998) Axin, an inhibitor of the Wnt-signalling pathway, interacts with β-catenin, GSK-3β and APC and reduces the β-catenin level. *Genes Cells*, **3**, 395–403.

Orford,K., Crockett,C., Jensen,J.P., Weissman,A.M. and Byers,S.W. (1997) Serine phosphorylation-regulated ubiquitination and degradation of β-catenin. *J. Biol. Chem.*, **272**, 24735–24738.

Peifer,M. (1995) Cell adhesion and signal transduction: the Armadillo connection. *Trends Cell Biol.*, **5**, 224–229.

Saito,Y., Vandenheede,J.R. and Cohen,P. (1994) The mechanism by which epidermal growth factor inhibits glycogen synthase kinase-3 in A431 cells. *Biochem. J.*, **303**, 27–31.

Sakanaka,C., Weiss,J.B. and Williams,L.T. (1998) Bridging of β-catenin and glycogen synthase kinase-3β by Axin and inhibition of β-catenin-mediated transcription. *Proc. Natl Acad. Sci. USA*, **95**, 3020–3023.

Schultz,J., Milpetz,F., Bork,P. and Ponting,C.P. (1998) SMART, a simple modular architecture research tool: identification of signalling domains. *Proc. Natl Acad. Sci. USA*, **95**, 5857–5864.

Siegfried,E., Wilder,E.L. and Perrimon,N. (1994) Components of Wingless signalling in *Drosophila. Nature*, **367**, 76–79.

Smalley,M.J., Titley,J. and O'Hare,M.J. (1998) Clonal characterisation of mouse mammary luminal epithelial and myoepithelial cells separated by fluorescence-activated cell sorting. *In Vitro Cell Dev. Biol. Animal*, **34**, 711–721.

Sokol,S.Y. (1996) Analysis of Dishevelled signalling pathways during *Xenopus* development. *Curr. Biol.*, **6**, 1456–1467.

Sokol,S.Y., Klingensmith,J., Perrimon,N. and Itoh,K. (1995) Dorsalizing and neuralizing properties of Xdsh, a maternally expressed *Xenopus* homolog of Dishevelled. *Development*, **121**, 1637–1647.

Stambolic,V. and Woodgett,J.R. (1994) Mitogen inactivation of glycogen synthase kinase-3β in intact cells via serine 9 phosphorylation. *Biochem. J.*, **303**, 701–704.

Staudinger,J., Lu,J. and Olson,E.N. (1997) Specific interaction of the PDZ domain protein PICK1 with the COOH terminus of protein kinase C-α. *J. Biol. Chem.*, **272**, 32019–32024.

Steitz,S.A., Tsang,M. and Sussman,D.J. (1996) Wnt-mediated relocalisation of dishevelled proteins. *In Vitro Cell. Dev. Biol.*, **32**, 441–445.

Strutt,D.I., Weber,U. and Mlodzik,M. (1997) The role of RhoA in tissue polarity and Frizzled signalling. *Nature*, **387**, 292–295.

Sussman,D.J., Klingensmith,J., Salinas,P., Adams,P.S., Nusse,R. and Perrimon,N. (1994) Isolation and characterisation of a mouse homolog of the *Drosophila* segment polarity gene Dishevelled. *Dev. Biol.*, **166**, 73–86.

Theisen,H., Purcell,J., Bennett,M., Kansagara,D., Syed,A. and Marsh,J.L. (1994) Dishevelled is required during Wingless signaling to establish both cell polarity and cell identity. *Development*, **120**, 347–360.

Willert,K., Brink,M., Wodarz,A., Varmus,H. and Nusse,R. (1997) Casein kinase 2 associates with and phosphorylates Dishevelled. *EMBO J.*, **16**, 3089–3096.

Yamamoto,H., Kishida,S., Uochi,T., Ikeda,S., Koyama,S., Asashima,M. and Kikuchi,A. (1998) Axil, a member of the Axin family, interacts with both glycogen synthase kinase-3β and β-catenin and inhibits axis formation of *Xenopus* embryos. *Mol. Cell. Biol.*, **18**, 2867–2875.

Yanagawa,S., van Leeuwen,F., Wodarz,A., Klingensmith,J. and Nusse,R. (1995) The Dishevelled protein is modified by Wingless signaling in *Drosophila. Genes Dev.*, **9**, 1087–1097.

Young,C.S., Kitamara,M., Hardy,S. and Kitajewski,J. (1998) Wnt-1 induces growth, cytosolic β-catenin and TCF/LEF transcriptional activation in Rat-1 fibroblasts. *Mol. Cell. Biol.*, **18**, 2474–2485.

Zeng,L. *et al.* (1997) The mouse Fused locus encodes Axin, an inhibitor of the Wnt signaling pathway that regulates embryonic axis formation. *Cell*, **90**, 181–192.